Exciting tin-oxo cages

Light-induced chemistry for nanopatterning

Haitjema, J.

Publication date
2020

Document Version
Other version

License
Other

CHAPTER 3

Photochemistry of tin-oxo cages in solution*

Abstract

n-Butyl tin-oxo cages with hydroxide counterions (TinOH) or acetate counterions (TinA) were exposed to deep ultraviolet (DUV) light (225 nm) in solution, after which the photoproducts were characterized. UV/Vis spectroscopy confirmed that Sn–C bonds are broken upon DUV exposure by detecting a decrease in absorbance from the $[\sigma^*_{\mathrm{Sn–C}} \leftarrow \sigma_{\mathrm{Sn–C}}]$ transitions. The quantum yield of Sn–C cleavage was determined to be 60−80% by UV/Vis experiments. The cleavage of Sn–C bonds in TinOH upon DUV exposure was confirmed further by ^{1}H NMR spectroscopy. This showed that the Sn–C bond cleavage is homolytic, by indirect detection of transient radicals with a spin trap. NMR spectroscopy also showed a decrease in integrals of *n*Bu protons from TinOH. Four main photoproducts were identified with 1D ^{1}H, 2D TOCSY, DOSY and selective TOCSY NMR spectroscopy: *n*-octane, 1-butene, 1-butanol and 1,1-dimethoxybutane (selectivity 79.1%, 6.0%, 6.2% and 7.9%, respectively). When the solution was deoxygenated before DUV exposure and volatile compounds were distilled, only *n*-octane and 1-butene were detected. This indicates that 1-butanol and 1,1-dimethoxybutane form upon reaction with dissolved oxygen. A quantitative NMR experiment was carried out in a quartz NMR tube, which was exposed to increasing amounts of DUV radiation. The quantum yield of Sn–C bond cleavage was determined to be at least 20%, based on the observed generation rate of photoproducts. This quantum yield may, however, be underestimated because a lot of light is lost by reflection on the cylindrical quartz NMR tube. Reaction mechanisms for product formation were proposed; it is clear that radical chemistry plays a major role in the photochemistry of TinOH.

*J. Haitjema, Y. Boeije, A.W. Ehlers, A. M. Brouwer, "Photochemistry of tin-oxo cages in solution", *Manuscript in preparation.*

3.1 Introduction

Understanding the photochemistry of tin-oxo cages is one of the main aims of the research discussed in this thesis. In this chapter, deep ultraviolet light (DUV, 225 nm) is used to expose tin-oxo cages in solution, followed by photoproduct analysis. While DUV photoreactions are different from EUV photoreactions, the generated excited states or photoproducts may be similar.[109] Moreover, EUV lithography machines may produce out-of-band radiation in the deep UV region, which could be detrimental to pattern resolution.[110] DUV photoreactions should therefore be understood to develop better EUV photoresists. In the ideal case, an EUV photoresist would respond only to EUV but not (or only very weakly) to DUV radiation.

Photoreactions that occur upon DUV exposure of tin-oxo cage thin films have been studied previously by X-ray photoelectron spectroscopy as well as UV/Vis spectroscopy.[102,111] It was shown that the solubility switch occurs upon exposure to DUV light as well. A photoreaction mechanism was proposed for this solubility switch, making a distinction between reactions performed under air and under nitrogen atmosphere (see Scheme 3.1). In both cases, DUV exposure led to the loss of carbon as a result of Sn–C bond cleavage. Under air atmosphere, immediate oxidation processes are possible, leading to a larger amount of oxygen in the photo-exposed tin-oxo cage product. Although EUV exposures are performed under either vacuum or reductive (H_2) atmosphere,[112] reactions with oxygen are still relevant on account of the post-exposure baking (PEB) step, which is usually performed in air. It is hypothesized that intermediary products react further during this step (see Chapter 2). These intermediary products have thus far not been firmly identified.

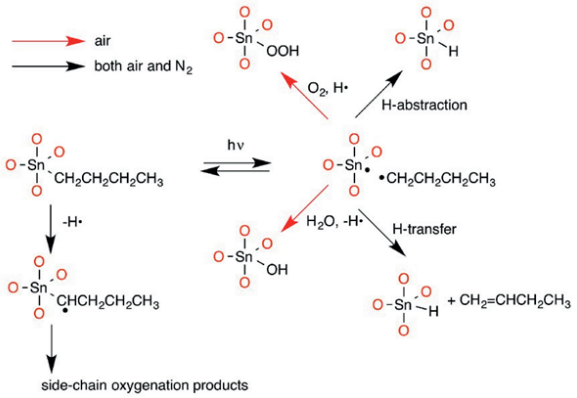

Scheme 3.1: Proposed photochemical reactions for TinOH thin films exposed to DUV in air and N_2, as proposed by Zhang and coworkers. Adapted from ref. 102.

Analyzing photoproducts and intermediates in thin films is challenging, because only a small amount of converted material is produced. Exposing in solution, followed by post-exposure analysis, significantly broadens the choice of spectroscopic

techniques.

One such method is UV/Vis spectroscopy. UV/Vis spectra of tin-oxo cage films show a broad absorption band ($\lambda_{max} \approx 220$ nm).[102] This absorption band decreased upon DUV exposure, indicating cleavage of Sn–C bonds and possible Sn–O bond formation. However, film inhomogeneity and roughness complicated quantification of the observed changes. In solution, the light exposure is distributed homogeneously because diffusion can take place and the solution can be stirred during exposure.

NMR spectroscopy can also be used to analyze the photoproducts. The chemical shifts (δ) and coupling constants (J) can provide unambiguous identification. Furthermore, NMR spectroscopic studies on tin-oxo cages are abundant,[89,99,107,113–117] providing a good starting point for analysis. 1D ^{1}H, ^{13}C and ^{119}Sn NMR have all been used for studies on tin-oxo cages. ^{13}C and ^{119}Sn NMR, however, have only low sensitivity and are therefore less suitable for photoproduct identification, although they can be used for confirmation of the starting material (TinOH). ^{1}H NMR is sufficiently sensitive for identification of photoproducts. This identification can be strengthened by more sophisticated NMR methods, such as TOtal Correlated SpectroscopY (TOCSY).

In ^{1}H–^{1}H 2D TOCSY, coupling between protons of the same "spin system" is observed.[118] Separation of signals is caused by a spin-lock in the pulse program, in which all the protons that are correlated to each other in sequence will get polarized and thus give a signal in the acquisition phase.[119] In the case of TinOH, the *n*Bu groups attached to 5-coordinated tin (Sn_5) and 6-coordinated tin (Sn_6) can be distinguished.

Selective TOCSY (or 1D TOCSY) is a method similar to 2D TOCSY, but the spectrum is obtained after selectively pulsing one proton signal. Accordingly, 1D spectra are obtained in which only the proton signals are seen that correlate to the specifically pulsed proton signal. In this way, overlapping signals in the 2D TOCSY can be easily separated by pulsing at different proton signals.

Diffusion Ordered SpectroscopY (DOSY) NMR is a method to distinguish differently sized particles in a sample. It is a pulsed field gradient NMR technique that separates each signal according to diffusion rate, and has been used to determine the associative behavior of tin-oxo cages.[89,115] It can also be used to study the size (hydrodynamic radius) of starting material and photoproducts.

The downside of solution exposure is that use of EUV light is not practical owing to the ultrashort absorption length of EUV in liquids. Therefore, only exposure to DUV (225 nm) was performed. Only a few solvents are sufficiently transparent in this spectral region; methanol (MeOH) and ethanol (EtOH) were chosen for the experiments, since tin-oxo cages can be readily dissolved in them.

Solution photochemistry is different from solid-state chemistry. For radical chemistry in solution, an important aspect is the "radical cage effect",[120,121] in which two formed radicals are surrounded by solvent molecules, making it difficult for the radicals to diffuse out of each other's vicinity. This effect explains why photodissociation yields are lower in solution than in the gas phase; in solution recombination of radicals is much more likely.[122] In the solid state, diffusion is even slower.[123,124] Therefore, it should be kept in mind that the quantum yield of photo-exposure in solution is expected to be higher than the quantum yield in a photoresist film.

3.2 Experimental

3.2.1 Synthesis

Tin-oxo cage materials were prepared as mentioned before (see Chapter 2).[88] The tin-oxo cage was prepared with tosylate counterions, after which the material was converted to hydroxide form (TinOH) by ion exchange using aqueous tetramethyl ammonium hydroxide.[114] Conversion to the acetate form (TinA) was performed by reacting TinOH with two molar equivalents of acetic acid.[89]

3.2.2 UV/Vis spectroscopy

For UV-visible samples, approximately 5–10 mg of TinOH or TinA were dissolved in 3 mL of solvent. This was then further diluted to achieve a final concentration of 1–10 μM in 3 mL. UV/Vis spectra were recorded using a Shimadzu 2700 spectrometer, using spectroscopic grade solvents (methanol, ethanol, cyclohexane, isopropanol). The spectra for quantitative analysis were baseline-corrected by setting the absorbance at 320 nm (far from the absorption band) to zero.

3.2.3 NMR spectroscopy

TinOH (21 mg ≈ 8.2 μmol) was dissolved in 1.8 mL of MeOH-d_4, leading to a concentration of approximately 4.6 mM. A solution of TinOH in deuterated solvent (4.6 mM) inside a 1×1 cm^2 quartz cuvette was exposed by a laser (see Section 3.2.4). After multiple time intervals, a sample was taken out of the cuvette to obtain an NMR spectrum after DUV exposure.

A quartz NMR tube was used for the quantitative NMR experiment. The sample was directly measured (no aliquots were taken), after which the sample was exposed to the next dose of DUV. In this experiment, 21 mg of TinOH powder was dissolved in 0.6 mL of MeOH-d_4.

1D ^{1}H NMR

1D ^{1}H NMR spectra were recorded on a Bruker AVANCE NEO 500 MHz spectrometer. The solvent used was MeOH-d_4 (Sigma Aldrich or VWR, ≥99.8 atom % D, ≥99% purity). At least 16 scans per sample were recorded, or more (up to 512) if low quantities of product needed to be detected. Typical concentration of tin-oxo cages was 5 mM (12 mg/mL).

1D ^{119}Sn NMR

1D ^{119}Sn NMR spectra were recorded on a Bruker AVANCE NEO 500 MHz spectrometer. The solvent was MeOH-d_4 (Sigma Aldrich or VWR, ≥99.8 atom % D, ≥99% purity) or CD_2Cl_2, measuring at least 2000 scans per sample. Typical concentration of tin-oxo cages was 60 mM (140 mg/mL).

1D/2D TOCSY

The same concentration was used as for 1D ^{1}H NMR. 1D and 2D TOCSY spectra were recorded on a Bruker AVANCE NEO 500 MHz spectrometer. Total Correlated Spectroscopy NMR (TOCSY-NMR) was performed based on a method by Bax and coworkers.[119] For 2D TOCSY, 16 scans were performed in the f1 direction and 256 scans were performed in the f2 direction, with a total measurement time of around 2 h. Spin-lock (mixing) time was 200 ms for all TOCSY experiments.

DOSY NMR

The same concentration was used as for 1D ^{1}H NMR. At the start of each diffusion-ordered spectroscopy (DOSY) experiment, the diffusion delay (D20) was tuned to get a clear signal at 98% gradient strength, and 2–3% of the signal at 2% gradient strength. The optimal value for D20 was found to be 0.12 s. Pulse duration (P30) was 0.5 µs for each scan.

Spectra were then recorded at 16 different gradient strengths (between 98 and 2%). Each spectrum was recorded 16 times. The result is an NMR spectrum in which the signals decrease as a function of gradient strength. This decrease was fitted to a mono-exponential decay function, with each peak having a different decay rate which is related to its diffusion constant. The fitting procedure was carried out using Bruker Dynamics software.

The diffusion axis of the DOSY plots was calibrated by using literature values for the self-diffusion constant of methanol ($\log(D) = -8.63$).[125] The chemical shift axis was calibrated by using a literature value for the chemical shift of the CH_3 groups in MeOH (3.34 ppm).[126]

Quantitative NMR

Quantitative NMR measurements were carried out in a quartz NMR tube, which was directly exposed to DUV irradiation. 21 mg of TinOH (8.5 µmol) were dissolved in 0.6 mL MeOH-d_4. iPrOH, which was already present in all prepared TinOH powders,[107] was used as an internal standard. It was assumed that all photons were absorbed by the solution, because of the high absorption coefficient of TinOH at 225 nm (approximately 10^5 $M^{-1}\,cm^{-1}$)[103] and high concentration, leading to an absorbance $A > 100$. The actual number of absorbed photons may be lower as a result of reflection losses.

Evans method

A stock solution of spectroscopic grade acetonitrile (MeCN, 0.1 mL) and TinOH (20 mg; 8.5 µmol) in MeOH-d_4 (2 mL) was prepared. 1 mL of this stock solution and 2,2,6,6-tetramethylpiperidinyloxyl ("TEMPO", 3.2 mg) were added to a 1 × 1 cm^2 quartz cuvette. 0.6 mL of this solution was added to a glass NMR tube and a glass capillary with stock solution (TinOH/MeCN in MeOH, but no TEMPO) was placed inside this tube, after which an ^{1}H NMR spectrum was obtained. After measurement, the solution was added back to the cuvette and the sample was exposed at 225

nm at multiple durations, while stirring at 400 rpm. After 1 h and 2 h of DUV exposure, ^{1}H NMR spectra were obtained. In each measurement the capillary with stock solution was placed inside the NMR tube. Two different blank experiments were performed to correct for the possible radical photochemistry of TEMPO independent of TinOH (blank 1) and the possibility that TinOH reacts with TEMPO without light absorption (blank 2). For blank 1, a stock solution of TEMPO in MeOH-d_4 (without TinOH) was prepared and the ^{1}H NMR spectrum of unexposed TEMPO as well as exposed TEMPO (1 h and 2 h) was measured. For blank 2, the same stock solution of MeCN and TinOH in MeOH-d_4 was prepared. ^{1}H NMR spectra were obtained at multiple time intervals of a solution of TEMPO (3.2 mg) and 1 mL stock solution (1 h and 2 h waiting time).

3.2.4 DUV exposures

DUV exposures were carried out using an Ekspla NT342B tunable laser system, using a wavelength of 225 nm. Pulse repetition rate was 10 Hz with a pulse width of 3–6 ns and typical pulse energy of around 1 mJ. The solution was stirred by a stirring bar (400 rpm) during exposure. Aliquots were taken out of the cuvette and transferred into NMR tubes.

3.2.5 Freeze-thaw technique and distillation

Selected samples of TinOH dissolved in MeOH-d_4 (1 mL of solution, approximately 5 mM) were deoxygenated before DUV exposure by using the freeze-pump-thaw technique. This was done using a custom-made setup in which a flask was connected to a quartz cuvette, in which gas and liquid flow can be controlled by various valves (see Fig. 3.1).

The flask with solution was frozen using liquid N_2 after which the atmosphere was pumped off ($p < 0.01$ mbar). The vacuum connection was closed and the solution was warmed to room temperature (water bath). After this, the flask was frozen and evacuated again, repeating the procedure three times. The deoxygenated solution was transferred to the cuvette for DUV exposure, without any exposure to oxygen. After exposure, the solution was transferred back to the flask for distillation. First, the flask was frozen (N_2) and the atmosphere was pumped off. The valve connecting to the vacuum was then closed and the flask was warmed to room temperature. At the same time, the setup was connected to an NMR tube which was cooled down using liquid N_2 and evacuated. The connection to the NMR tube was then opened, after which volatile compounds condensed in the NMR tube.

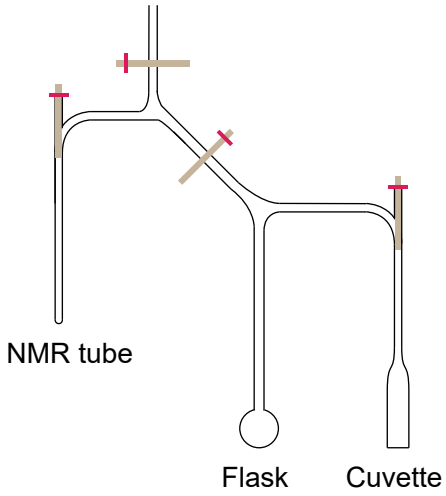

Figure 3.1: Schematic representation of the setup used for the freeze-thaw cycle (deoxygenation), followed by DUV exposure and distillation.

3.3 Results and discussion

3.3.1 UV/Vis spectroscopy

UV-visible (UV/Vis) spectroscopy is a useful tool to track chemical (photo)-reactions of tin-oxo cages in solution. It has the advantage of high sensitivity, being able to detect species at very low concentrations (micromolar or even lower).

The DUV photochemistry of TinOH primarily arises from [σ^* ← σ Sn–C] transitions, which give rise to a collective absorption maximum (λ_{max}) around 220 nm. In these transitions, an electron is promoted from the sp^3-hybridized Sn–C bond, mostly at the 6-coordinated tin atom, to an empty σ^* orbital.[103] The calculations show that this excited state also has significant σ^* Sn–C character. This electronic transition weakens the Sn–C bond, leading to bond cleavage. Therefore it is expected that the intensity of the [σ^* Sn–C ← σ Sn–C] transition will decrease upon DUV exposure. Since fewer transitions are available and the transition moments are smeared out over multiple transitions, the absorption band corresponding to the [σ^* Sn–C ← σ Sn–C] transitions broaden and decrease in intensity.

UV-visible spectra of unexposed TinOH

First, UV/VIS absorption spectra were obtained from unexposed samples of TinOH in methanol (MeOH), isopropanol (iPrOH) and cyclohexane (cHex) and show a strong absorption near 220 nm with a molar absorption coefficient $\epsilon \sim 10^5$ M^{-1} cm^{-1} (see Fig. 3.2). A red shift is observed moving from the most polar solvent (MeOH) to the least polar (cHex). UV/Vis spectra of other tin-oxo cages, such as TinA, show a very similar absorption band (see below).

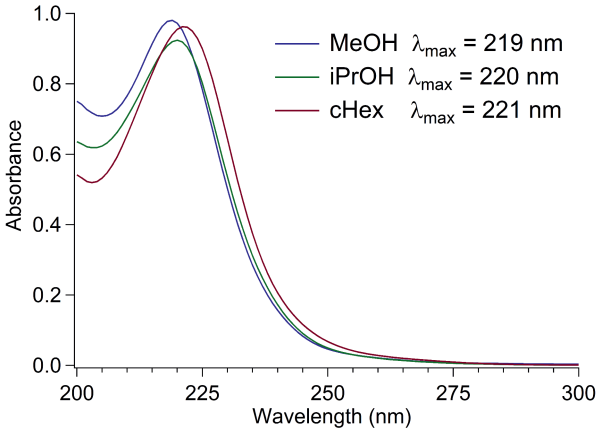

Figure 3.2: UV/VIS Absorption spectra of TinOH in MeOH (blue), iPrOH (green) and cHex (red). Concentrations are 9.1 µM. $\epsilon \sim 10^5$ M^{-1} cm^{-1} at λ_{max}.

UV-visible spectra of DUV-exposed tin-oxo cages

Tin-oxo cages were irradiated in solution, after which the UV/Vis spectrum was measured. The results are shown in Fig. 3.3. These experiments were done on TinA (acetate counterions) in spectroscopic ethanol. The used materials therefore deviate slightly from the NMR experiments shown later in this chapter, which were performed in a solution of TinOH in methanol. In the ESI (Fig. 9.2), UV/Vis results for photo-exposure of TinOH in methanol are also shown; the results are very similar to those shown in Fig. 3.3. In the absorption band, the absorbance A decays with increasing exposure dose D, as can be seen in Fig. 3.4. This decay can be described as mono-exponential:

$$A = a + be^{-cD} \tag{3.1}$$

where a, b and c can be obtained by fitting. a can be viewed as the absorbance value at infinite exposure dose. b is a scaling factor and c gives the rate at which the absorbance decreases (in mJ^{-1}).

a is clearly not zero, which means that even at exceedingly high doses, there is still absorption remaining. This can be explained in two ways. First, other transitions could

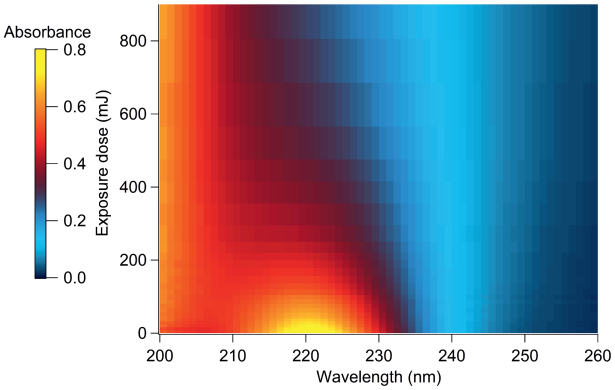

Figure 3.3: UV/Vis absorption spectra of TinA (6.9 μM in EtOH) as a function of exposure dose.

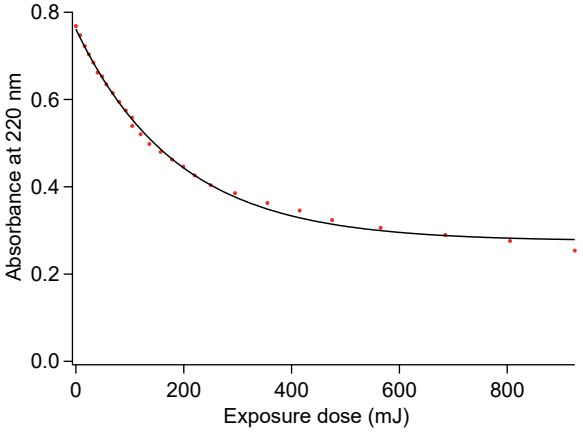

Figure 3.4: Absorption at 220 nm plotted vs. DUV (225 nm) irradiation dose, for 3 mL of a 6.9 μM solution of TinA (tin-oxo cage with acetate counterions) in EtOH. Fitted to function $A = a + be^{-cD}$, with $a = 0.28$, $b = 0.49$ and $c = 5.3 \times 10^{-3}$ mJ^{-1}.

give rise to absorption at 220 nm which do not lead to Sn–C cleavage, and therefore no decrease in absorption. This gives rise to a background a. Secondly, photoproducts can also be formed that give rise to absorption. This would also give rise to an apparent decrease in the rate c and a background a. It should be noted that formation of photoproducts normally does not lead to bi-exponential behavior, because the rate of photoproduct formation will usually be equal to the rate of irreversible Sn–C cleavage. Because both these explanations have a similar effect, they are difficult to separate from each other; both are probably correct.

DUV-induced conversion of tin-oxo cages to photoproducts can be studied quantitatively. Both the initial amount of tin-oxo cage and the number of absorbed photons are known. The latter can be calculated from the laser power ($\sim$ 10 mW) and the absorbance values.

In a simple approximation, the strength of the absorption band ($\lambda_{\text{max}} \approx 220$ nm) scales linearly with the number of Sn–C bonds present and the DUV source is monochromatic. This approximation may be the most valid at short exposure times (0–60 sec.), because only small amounts of products are generated in this case.

The number of absorbed DUV photons can be approximated by Eq. 3.2:

$$N_{\text{photons}} = \frac{P \cdot t \cdot (1 - 10^{-\bar{A}})}{E_{\text{phot}}} \tag{3.2}$$

In Eq. 3.2, P is the laser power (in Watt), t is the exposure time (s), $\bar{A}$ is the average absorbance during exposure, and E_{phot} is the energy of one DUV photon (8.8×10^{-19} J, as given by $\frac{hc}{\lambda}$). $\bar{A}$ can be approximated by taking the average of the absorbance between dose 0 and dose D_1. The average value of a function in the interval between x_0 and x_1 is given by:

$$\frac{1}{x_0 - x_1} \int_{x_0}^{x_1} f(x)\, dx \tag{3.3}$$

Substituting 3.1 for $f(x)$, the exposure dose D_1 for x_2, and 0 for x_1, we obtain:

$$\begin{aligned} \bar{A} &= \frac{1}{D_1} \int_0^{D_1} a + b\mathrm{e}^{-cD}\, dD \\ &= a + \frac{b}{cD_1} - \frac{b}{cD_1}\mathrm{e}^{-cD_1} \end{aligned} \tag{3.4}$$

In Eq. 3.4, D is the exposure dose and D_1 is the exposure dose at which the number of absorbed photons is evaluated. a, b and c are fit parameters, obtained by fitting the absorbance vs. exposure dose plot to an exponential decay. The number of photochemical events (Sn–C bond cleavage in this case) can be calculated by Eq. 3.5:

$$N_{\text{Sn–C bond cleaved}} = (n_0 - n) \cdot N_{\text{A}} \cdot 12 \tag{3.5}$$

In Eq. 3.5, n is the amount of TinOH (in mol) at time t, n_0 is the amount of TinOH for the unexposed material, and N_{A} is Avogadro's number. The factor 12 appears because each TinOH molecule contains 12 Sn–C bonds.

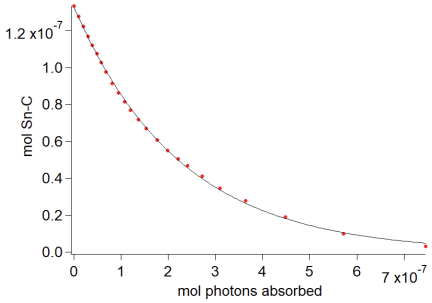

Figure 3.5: Mol Sn–C bonds plotted vs. the number of absorbed photons for 3 mL of a 6.9 µM solution of TinA in EtOH. The number of Sn–C bonds was corrected for baseline absorption. The fitted curve is an exponential decay: $a + be^{-cD}$ with $a = 0$, $b = 1.3 \cdot 10^{-7}$ mol, $c = 4.9 \cdot 10^{6}$ mol^{-1}.

For an initial TinA concentration of 6.9 µM, $a = 0.28$, $b = 0.49$, and c is 5.3×10^{-3} mJ^{-1}. Using the integration procedure described in Eq. 3.4, the absorbed dose can be calculated for each data point. This can be plotted vs. the remaining number of Sn–C bonds (see Fig. 3.5), which can be calculated using the molar concentration of tin-oxo cage and the total volume of the solution (3 mL).

One would expect Fig. 3.5 to show a linear decay, since each absorbed photon is expected to break a fixed number of Sn–C bonds (the quantum yield). This is clearly not the case; the plot again shows a mono-exponential decay. This means that the quantum yield decreases with increasing exposure dose. This can be explained by the loss of Sn–C over time, which means that an increasing number of photons that are absorbed do not cause Sn–C cleavage and do not lead to a decrease in absorption.

To determine the quantum yield, it is the most reasonable to choose the slope at zero dose. In this case, no other products are formed yet that complicate the analysis. The quantum yield is then given by the derivative at $D = 0$, which is $-bc$ in case of an exponential decay ($a + be^{-cD}$).

The quantum yield as calculated is shown for different samples of TinA with different concentrations. At higher tin-oxo cage concentration the quantum yield appears to be higher, as shown in Fig. 3.6. This could indicate a reaction with other tin-oxo cages after exposure, which would become more probable as the concentration increases. However, this conclusion is only preliminary on account of the limited number of data points.

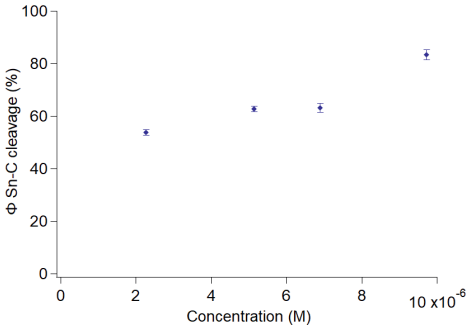

Figure 3.6: Quantum yield Φ of Sn–C cleavage as function of TinA concentration. Concentration was calculated using the absorption spectrum and the molar absorption coefficient. Error bars are standard deviations, as calculated using the standard deviation obtained from the fitting procedure and the "propagation of errors" formula (see Chapter 6).

3.3.2 NMR spectroscopy on unexposed material

NMR spectroscopy yields much more structural information on photoproducts than UV/Vis spectroscopy. To study DUV-induced changes on tin-oxo cages in solution, a clear understanding of spectra of non-exposed tin-oxo cage is necessary. In various previous works, NMR studies on the tin-oxo cage have already been conducted. This includes ^{119}Sn NMR, ^{13}C NMR, ^{1}H NMR, DOSY NMR, etc.[89,99,107,113–115]

^{119}Sn NMR

Sn NMR is a useful tool to probe the chemical structure of organotin compounds, and is therefore commonly used in organotin chemistry.[127] ^{119}Sn NMR spectra of TinOH and TinOTs can be found in the ESI (Fig. 9.3 and 9.4). These spectra are in agreement with the literature.[114]

^{1}H NMR

In Fig. 3.7 the ^{1}H NMR spectrum of unexposed TinOH in MeOH-d_4 is shown. 2D TOCSY NMR (Fig. 3.8) was used for signal assignment. The spectrum and assignment are in agreement with the literature.[107] A detailed analysis of the ^{1}H NMR spectrum can be found in the ESI (Section 9.3.2). A small impurity of tetramethyl ammonium ions (TMA, a leftover from the synthesis, see Section 3.2.1) is detected at 3.2 ppm, but the compound is otherwise pure.

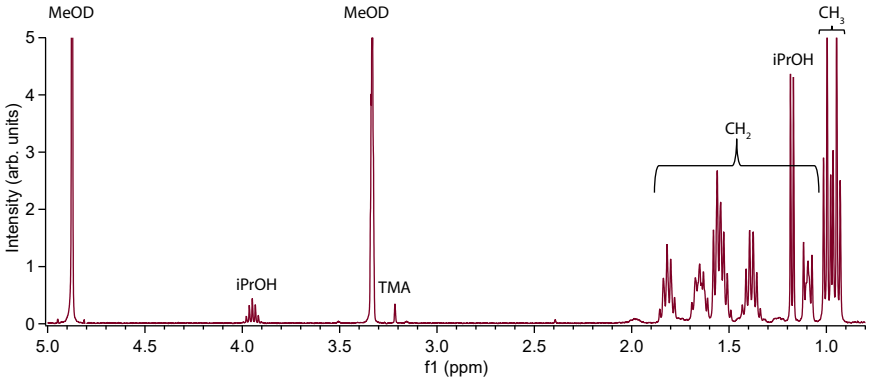

Figure 3.7: 400 MHz ^{1}H NMR spectrum of TinOH in MeOH-d_4.

2D TOCSY NMR

TOCSY is an NMR method that creates couplings between all protons within a "spin system", a chain of nuclei in which each is coupled to its neighbor.[118] Even protons at large distances can couple to each other. The 2D TOCSY spectrum of unexposed TinOH in MeOH-d_4, including the assignments, is shown in Fig. 3.8. This spectrum is zoomed-in on the *n*Bu region, where all the ^{1}H–^{1}H couplings are expected. The couplings between a chemically distinct group of *n*Bu protons can easily be derived by looking at one F2 peak and see which cross peaks on the F1 axis below that peak belong to that F2 signal. For example, starting right above on the F2 axis, Sn_6-CH_2-CH_2-CH_2-**CH_3** is found at 0.92 ppm as was found in the ^{1}H spectrum (Fig. 3.7). By scanning down the F1 axis, it can be seen that these methyl protons couple to signals at 1.07 ppm, 1.36 ppm and 1.63 ppm. This shows that with TOCSY only shows couplings between protons of the same *n*Bu. A table showing all couplings is shown in the ESI (Tab. 9.3).

Selective TOCSY

In a selective TOCSY experiment, a specific proton signal is pulsed. This leads to suppression of all signals that are not coupled to the proton signal via the "spin system". The selective TOCSY spectrum of unexposed TinOH in MeOH-d_4 is shown in Fig. 3.9, for two different pulsed signals. In the blue spectrum (top), Sn_6-CH_2-**CH_2**-CH_2-CH_3 at 1.63 ppm is pulsed, causing all the signals corresponding to the *n*Bu chain bound to the six-coordinated tin atom to evolve, while suppressing all the Sn_5 signals. In the green spectrum (middle), Sn_5-CH_2-**CH_2**-CH_2-CH_3 is pulsed, leading to suppression of all signals that do not correspond to this butyl chain. The red spectrum (bottom) is the normal ^{1}H spectrum, which is approximately the sum of the green and blue spectra, with an added signal for iPrOH.

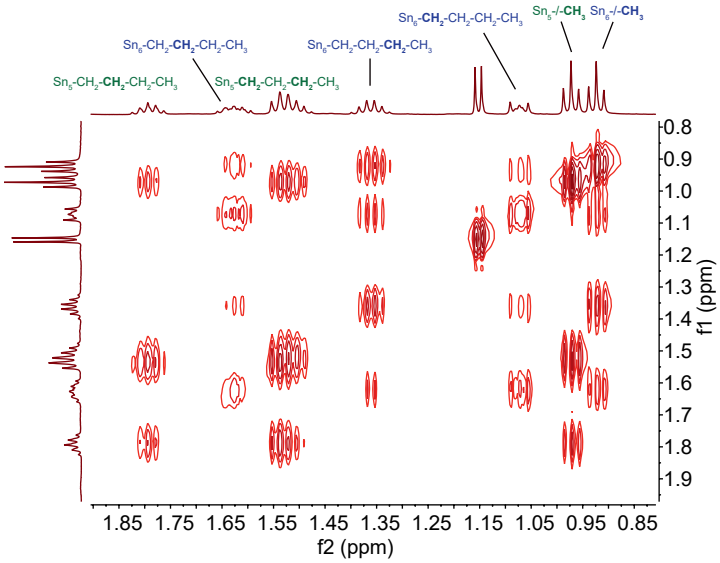

Figure 3.8: 500 MHz 2D TOCSY spectrum of TinOH in MeOH-d_4, zoomed-in on the nBu region. The assignments are shown as well.

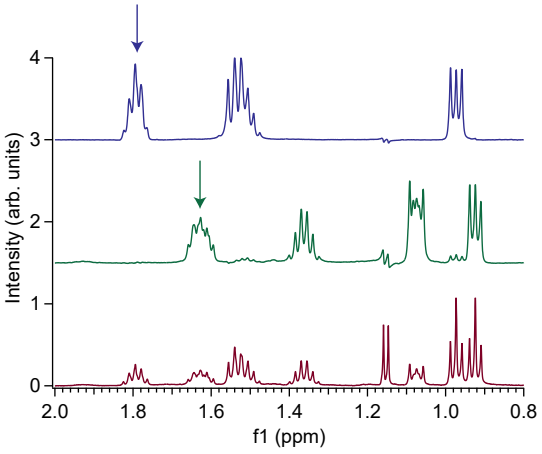

Figure 3.9: 500 MHz selective TOCSY spectra of TinOH in MeOH-d_4. Red: ^{1}H spectrum. Green: pulsed at 1.63 ppm (indicated with green arrow). Blue: pulsed at 1.79 ppm (indicated with blue arrow). A vertical offset was used on the y-axis.

3.3.3 Evans method: NMR spectroscopy and spin trapping

Cardineau and coworkers hypothesized first that the photochemistry of tin-oxo cages involves the formation of radicals after homolysis of Sn–C bonds, based on a mild correlation between EUV photosensitivity and strength of Sn–C bonds.[88] Quantum chemical calculations support the breaking of the Sn–C bond as the primary process after DUV photon absorption.[103] Zhang and coworkers performed DUV radiation induced solid-state chemistry of tin-oxo cage films, followed by XPS analysis.[102] From these results mechanistic pathways were suggested, which involved initial homolytic bond cleavage. However, this has not been definitively proven, because the volatile reaction products could not be identified yet.

In this work, the Evans method was used to demonstrate formation of transient radicals upon photon absorption by TinOH.[128] This method is based on the dependence of the NMR chemical shift of reference compounds on the concentration of unpaired electrons (paramagnetic species) in a sample. These unpaired electrons have an interaction with the hydrogen nuclei of the reference compound, changing the chemical shift of its signal. Both the contact interaction and the dipolar interaction between the unpaired electron and nucleus are involved in this paramagnetic shifting.[129] Besides the shift, paramagnetic species decrease the relaxation times of protons, significantly broadening all signals.

The paramagnetic shift of the reference compound scales linearly with the concentration of paramagnetic species. By observing the frequency difference (Δf) of a resonance in the presence and absence of paramagnetic species, the magnetic susceptibility (χ_m) can be obtained. This is quantified in Eq. 3.6.

$$\chi_\mathrm{m} = \frac{3\Delta f}{4\pi F c} \tag{3.6}$$

In Eq. 3.6, χ_m is the magnetic susceptibility (mL/mmol), Δf is the frequency difference between the shifted resonance and the pure solvent resonance (Hz), F is the spectrometer radiofrequency (Hz), and c is the concentration of paramagnetic species (mmol/mL).

The frequency difference between shifted resonance and the pure solvent resonance can be measured directly, using a capillary (reference) within an NMR tube (see Fig. 5.2a). The NMR tube contains a paramagnetic substance that shifts the signal, while the capillary does not and shows a signal which is not paramagnetically shifted. The NMR spectrum shows a shift in ppm value ($\Delta\delta$) which can be converted to Δf using the spectrometer frequency.

The measurement of transient radicals is limited by the short lifetime of radical species. In an ideal case, the radical species are measured *in situ*. In our case, however, it would involve intersecting a DUV light source with an NMR spectrometer, which for practical reasons was not possible. A way to prove formation of radicals after they have terminated is through the use of spin traps that selectively react with radicals. In this work, the paramagnetic spin trap TEMPO was used (Fig. 5.2b), which contains an unpaired electron at the oxygen atom but is sufficiently stable.

TEMPO converts to a stable diamagnetic species upon reaction with a radical.

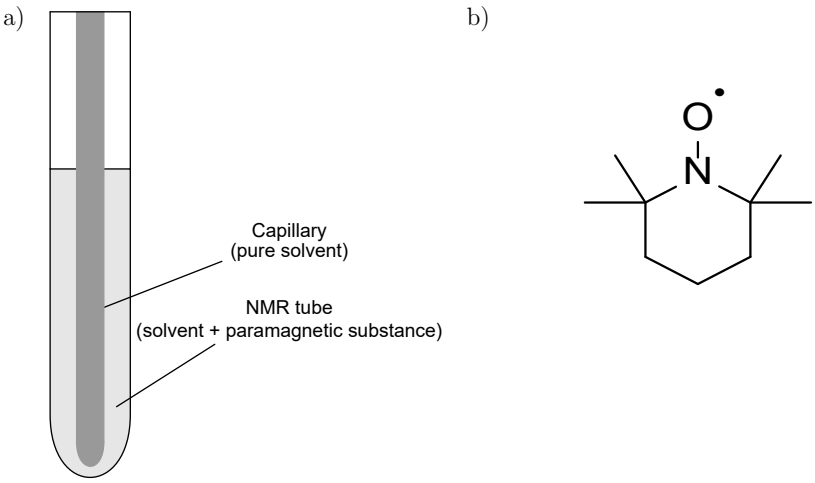

Figure 3.10: (a) Schematic representation of the Evans method, (b) chemical structure of the spin trap used (2,2,6,6-Tetramethylpiperidin-1-yl)oxyl (TEMPO).

The larger the amount of TEMPO, the larger the shift (Δf) between the capillary and NMR-tube signals. If this shift decreases upon DUV exposure, this indicates a radical mechanism in the photochemistry of TinOH. In addition, the number of generated radicals can be quantified if the initial amount of TEMPO is known.

In our experiments, acetonitrile (MeCN) was used as a reference compound, because it is both chemically inert and transparent to DUV light. The chemical shift of a TinOH/MeCN solution in MeOH was then compared to a TinOH/MeCN/TEMPO solution in MeOH that was exposed to DUV light (225 nm), using a sealed capillary within an NMR tube. In Fig. 3.11, the resulting ^{1}H NMR spectra are shown, with increasing DUV exposure. In all spectra, two resonances corresponding to MeCN are shown. The larger peak corresponds to the signal in the capillary, which is not paramagnetically shifted. The smaller peak corresponds to the signal in the NMR tube, which is affected by paramagnetic shifting by TEMPO. Clearly, the paramagnetic shift is decreasing upon DUV exposure, indicating loss of paramagnetic species. This can be explained by the reaction of TEMPO with radicals arising from the DUV photochemistry of TinOH.

This reasoning is explained further in Fig. 3.12. Upon DUV exposure two radicals are expected to be created: a tin-centered radical and a butyl radical. As a spin trap, TEMPO can react with one of these highly reactive radicals, leading to a decrease in concentration of TEMPO. It is expected that TEMPO reacts faster with butyl radicals than with the bulkier tin-centered radicals. Upon DUV exposure, a triplet at 3.8 ppm is evolving, which indeed indicates the formation of a butyl-TEMPO adduct. The CH_2 protons adjacent to oxygen in this adduct are expected to appear at this chemical shift.[130] The other NMR peaks of the butyl-TEMPO adduct are

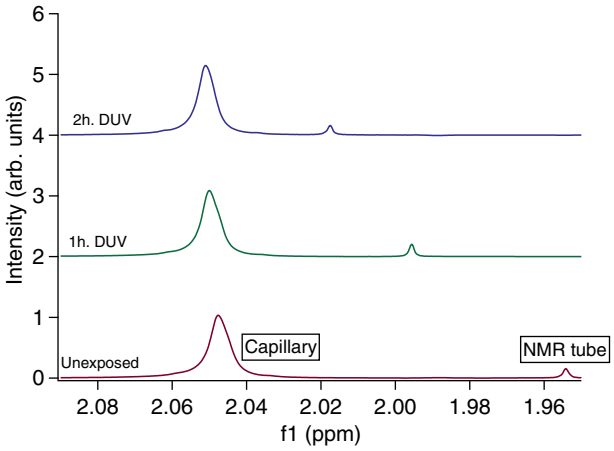

Figure 3.11: Evans method: ^{1}H NMR spectra of DUV exposed TinOH and TEMPO in MeOH-d_4, using MeCN as a reference. Bottom: unexposed. Middle: 1 h DUV exposed. Top: 2 h DUV exposed. $\Delta\delta = 0.035$ ppm after 1 h, 0.055 ppm after 2 h).

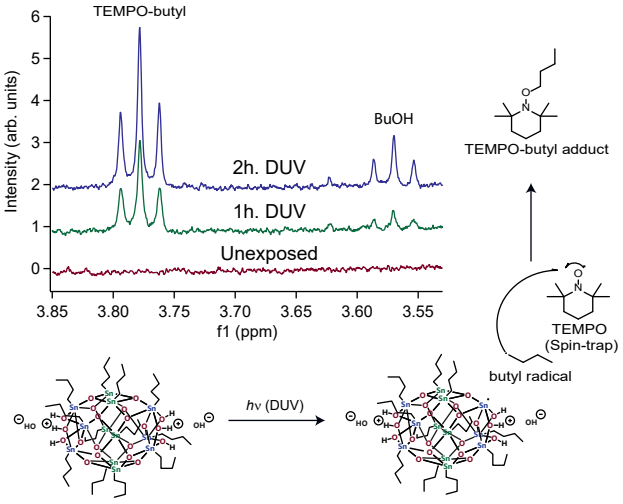

Figure 3.12: Spin-trapping of butyl radical with TEMPO and ^{1}H NMR measurement of formed TEMPO-adduct. A vertical offset was used on the y-axis.

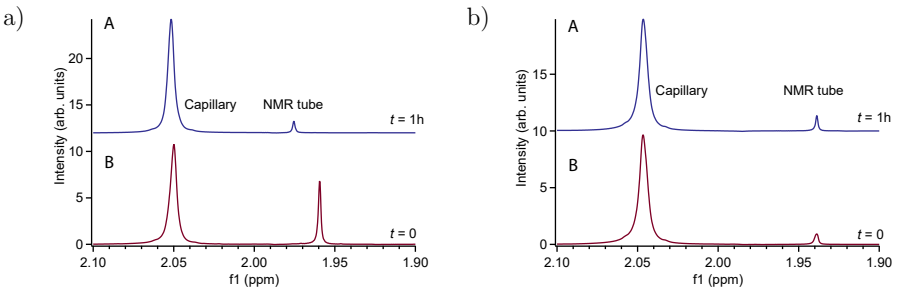

Figure 3.13: Blanks Evans Method. (a) Blank 1 (solution of TEMPO and MeCN in MeOH-d_4), without TinOH. Blue: 1 h DUV exposed. (b) Unexposed. $\Delta\delta$ (MeCN) = 0.01 ppm. Right: Evans Method (solution of TinOH, TEMPO and MeCN in MeOH-d_4), without DUV exposure. A (blue): $t = 1$ h. B (red): $t = 0$. $\Delta\delta$ (MeCN) = 0 ppm). Vertical offsets were used on the y-axes.

obscured by TinOH proton peaks. In addition, a large singlet at 1.14 ppm is appearing upon DUV exposure, which represents the methyl protons of a TEMPO adduct (see ESI, Fig. 9.7).[131] This confirms the loss of TEMPO radical upon DUV exposure and the formation of a diamagnetic TEMPO adduct. The presence of this adduct after exposure is a strong confirmation of the radical mechanism. Without TEMPO, the discussed peaks do not show up in the spectrum.

Tin-centered radicals could in principle react with TEMPO as well. However, this TEMPO-adduct was not detected by ^{1}H NMR spectroscopy. Its formation is likely sterically hindered. The tin-centered radicals are apparently unstable, as they do not contribute to the paramagnetic shielding. One possibility is that they decompose by breaking a second Sn–C bond to give a closed-shell tin compound and another Bu·, which is trapped by TEMPO.

In Fig. 3.12, it can also be seen that a triplet at 3.55 ppm is evolving. As shown below (Section 3.3.4), this signal corresponds to 1-butanol, which is a photoproduct after DUV absorption of TinOH.

To ensure that the decrease in TEMPO radical is caused by the photochemistry of TinOH, two blank experiments were performed. Blank 1 (without TinOH) checks the possibility of the radical photochemistry of TEMPO itself. As shown in Fig. 3.13a, there is a small difference in the peak distances from MeCN before and after exposure of $\Delta\delta = 0.01$ ppm. TEMPO thus appears to have a DUV photochemistry on its own, forming a diamagnetic species. However, this change in frequency difference is much smaller than the frequency shift seen in the photochemistry of TinOH ($\Delta\delta = 0.035$ ppm, see Fig. 3.11). Blank 2 (Fig. 3.27b) is the Evans experiment performed without DUV exposure, using a waiting time of 1 h. As can be seen, no paramagnetic shift occurs, which means that DUV irradiation must cause the paramagnetic shift.

In Table 3.1, the results from Figure 3.11 are quantified using Eq. 3.6. From Δf and the known starting concentration of TEMPO (11.3 mM), the concentration of TEMPO at different exposure times can be calculated. In this calculation, Δf of

Table 3.1: Frequency shifts for MeCN and corresponding conversion derived from Evans Method spectra in Fig. 3.11 and Eq. 3.6

DUV exp. (h)	**$\Delta\delta$ MeCN (ppm)**	**Δf MeCN (Hz)**	**Conc. TEMPO (mM)**	**Sn–*n*Bu conversion[a] (%)**
0	0.090	36.0	11.3	0
1	0.065	26.0	8.16	5.5
2	0.050	20.0	6.28	8.9

[a]Assuming conversion of one TEMPO molecule per Sn–*n*Bu.

TEMPO (Blank 1) is corrected for by extracting the shifts in this blank for 1 h of DUV exposure and extrapolating to 2 h of DUV exposure. Then, the conversion of the total number of *n*Bu chains from TinOH can be calculated with the known starting amount (8.5 µmol; 102 µmol *n*Bu), by assuming every TEMPO molecule has reacted with a cleaved butyl radical. In this way, it has been calculated that 5.5% of all Sn-*n*Bu chains have been converted after 1 h of DUV exposure, and 8.9% after 2 h. Using the laser power, we can calculate a quantum yield Φ (converted Sn–C bonds per photon). This was found to be 0.54%. In this calculation, it is assumed that every TEMPO molecule that has been converted to a diamagnetic species reacts with a *n*Bu radical from TinOH. However, the generated *n*Bu radicals can also react with the solvent or with each other. Furthermore, tin-centered radicals could contribute to the loss of TEMPO by generation of radicals (e.g. by H-atom abstraction) which could react with TEMPO. Therefore, Φ could be underestimated. Nevertheless, the Evans method has clearly proven the homolytic cleavage of Sn–C upon DUV exposure.

3.3.4 DUV exposure and product analysis by NMR

1D ^{1}H NMR

In Fig. 3.14, NMR spectra of unexposed and exposed solutions of TinOH in MeOH-d_4 are shown. Clearly, new signals appear in the NMR spectrum, which correspond to photoproducts. These are 1,1-dimethoxybutane ("acetal") at 4.49 ppm (t), 1-butanol at 3.55 ppm (t), and *n*-octane at 1.3 ppm (multiplet) and 0.88–0.91 ppm (triplet). Further, some low intensity signals can be observed at 9.70 ppm (butyraldehyde), 5.86 ppm (1-butene), 5.42 ppm, 4.98 ppm (1-butene), 2.41 ppm (butyraldehyde), 2.19 ppm and 2.06 ppm (1-butene) upon long exposure (see ESI, Fig. 9.8). Reference spectra were taken after short exposure times (on the order of minutes) to ensure that these product peaks also appeared after short exposure (i.e. they are not secondary products). Evidence for signal assignment will be shown in the upcoming discussion.

1-Butanol (BuOH) and butyraldehyde could be formed by reaction of formed Bu· with dissolved oxygen. This reaction is known from previous literature.[132,133] The

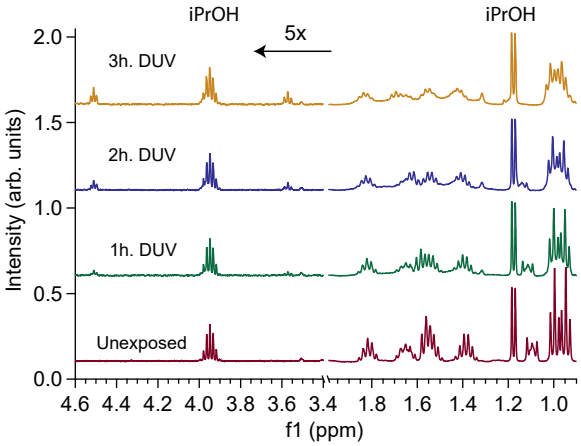

Figure 3.14: Zoomed-in 400 MHz ^{1}H NMR spectra of TinOH in MeOH-d_4 after multiple DUV exposure times. From bottom to top: 0 h (red), 1 h (green), 2 h (blue) and 3 h (purple) DUV exposure. The intensity in the left part of the graph was multiplied by five to show the product formation clearly. The spectra were normalized to the iPrOH C–H peak (3.95 ppm). A vertical offset was used on the y-axis.

intermediate peroxide BuOOH could be formed in this reaction, which could react further to form BuOH or butyraldehyde (see Scheme 3.2).[134] Butyraldehyde could further react with MeOH-d_4 to form the acetal 1,1-dimethoxybutane-d_6. This reaction is possibly catalyzed by TinOH (see below).

n-Octane and 1-butene are probably formed by reaction of butyl radicals with the formed Sn· or butyl attached to the tin-oxo cage (see Scheme 3.3). A tin (II) compound is formed if a butyl is abstracted by the initially formed butyl radical, while a tin hydride is formed if the tin radical abstracts a hydrogen atom from a butyl radical. Tin hydrides were not observed in the ^{1}H NMR spectrum, which could be due to their short lifetime.

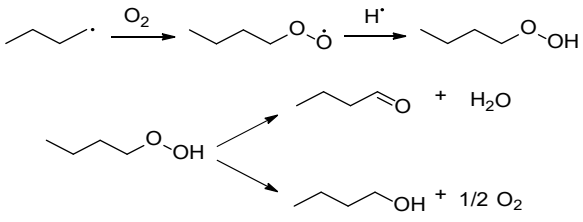

Scheme 3.2: Generation of BuOOH (top), a precursor to BuOH or butyraldehyde (bottom).

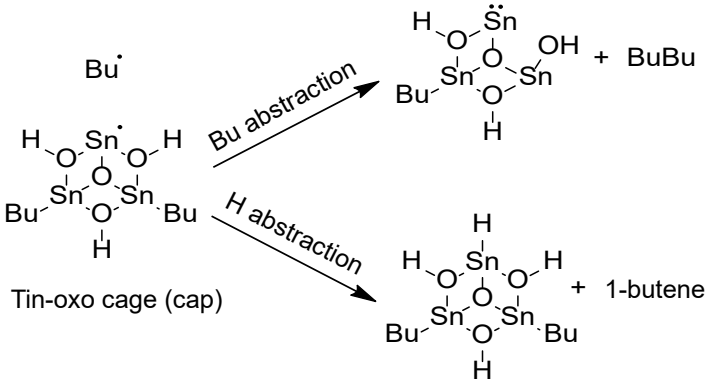

Scheme 3.3: Formation of *n*-octane (BuBu) by butyl abstraction by Bu· (top), and formation of 1-butene by H abstraction (bottom), at the cap of the tin-oxo cage (6-coordinated tin atoms). Each tin atom is bound to two more oxygen atoms, which have been omitted for clarity. The initial radical pair is formed by photodissociation.

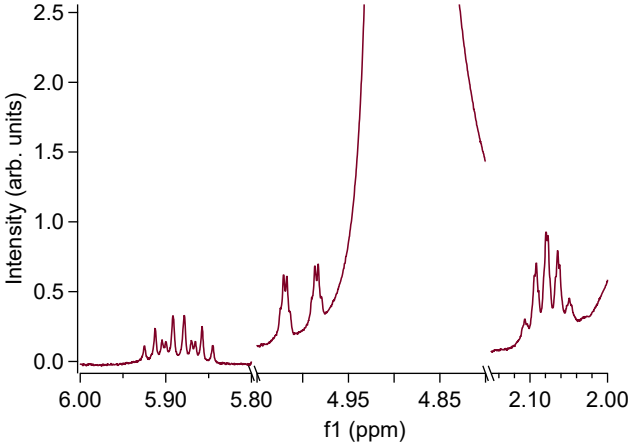

Figure 3.15: 500 MHz ^{1}H NMR spectrum of 2 h DUV exposed TinOH in MeOH-d_4, zoomed-in to show 1-butene peaks.

When zoomed in on the alkene region and acquiring the 1D spectrum after DUV exposure with 512 scans on a 500 MHz NMR spectrometer, 1-butene can be assigned unambiguously as shown in Fig. 3.15 (a full assignment, including coupling constants, is shown in the ESI, Tab. 9.5).[135] Two signals of 1-butene, at 4.90 and 1.00 ppm, are not visible because they overlap with other signals. The signal at 4.90 can be made visible by cooling the sample down to –80 °C, shifting the CD_3OH peak significantly downfield (see ESI, Fig. 9.10).

The *n*Bu peaks all broaden, decrease in intensity and shift slightly downfield. This shows that cleavage of Sn-*n*Bu bonds from the tin-oxo cage is occurring upon DUV absorption. Although calculations suggest that the *n*Bu is cleaved off primarily at the six-coordinate tin atoms,[103] the decrease in intensity of five-coordinated *n*Bu chain signals shows that chemistry is clearly occurring at the five-coordinated tin atoms as well.

The downfield shift is especially pronounced for the Sn_6-$\mathbf{CH_2}$-CH_2-CH_2-CH_3 signal (initially at 1.1 ppm), which at 2 h of DUV exposure overlaps with the iPrOH signal and at 3 h DUV exposure is partially downfield from this iPrOH signal. It is tempting to assign this shifted peak to a butyl chain bound to a Sn_6 atom at which some chemical change (such as a nearby butyl cleavage) has occurred. However, in such case there would be two Sn_6-$\mathbf{CH_2}$-CH_2-CH_2-CH_3 signals, one for unconverted and a shifted signal for converted TinOH. This is clearly not the case. Therefore, the downfield shift of the *n*Bu peaks is likely due to a changed chemical environment, induced by photochemical reactions. The coordination of solvent and/or pH changes after DUV exposure could influence the chemical shift of *n*Bu protons. In addition, rapid exchange of butylstannoic acid (Sn–BuOOH) between tin-oxo cages could occur, leading to an NMR signal that is averaged out.

Upon DUV exposure white insoluble material started to form. These white particles did not dissolve in either polar (H_2O) or non-polar (*n*-hexane) solvents. This could indicate the formation of agglomerated tin-oxo cages.

A control experiment (without exposure) was performed to ensure that the changes in NMR signals arise from the photochemistry. The sample was also stirred the same way as in the photochemistry experiments. The ^{1}H NMR spectrum did not show any significant difference after 2 hours of waiting time (see ESI, Fig. 9.6).

Distillation of volatile photoproducts

The NMR spectrum of DUV-exposed tin-oxo cages contains both photoproduct and tin-oxo cage signals. These signals partly overlap, which complicates product identification. A way to separate photoproducts from remaining tin-oxo cages is distillation. Photoproducts such as 1-butanol, 1-butene, *n*-butane and *n*-octane are volatile, whereas tin-oxo cages are not. Therefore, we performed distillation after exposing tin-oxo cages to DUV in solution (see Section 3.2.5 for details). A custom-made setup (see Fig. 3.1) was used to distill after exposure without exposing the solution to air. The setup also enabled deoxygenation prior to exposure, using the freeze-thaw cycle. In this way, reaction pathways that involve oxygen are excluded.

In Fig. 3.16, the spectrum of distilled volatile photoproducts is shown. Because

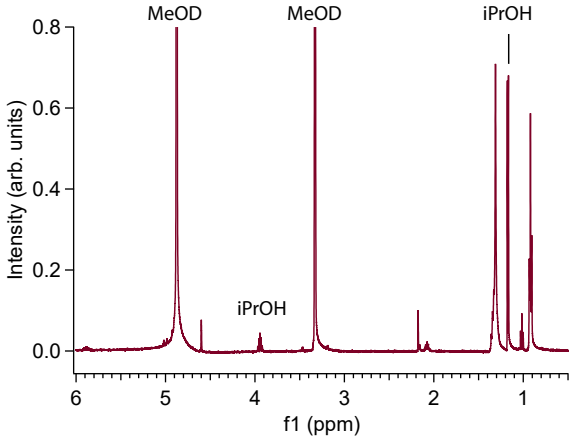

Figure 3.16: 500 MHz ^{1}H NMR spectrum of TinOH in MeOH-d_4, exposed to 45 min. of DUV radiation and distilled. Formed photoproducts are 1-butene (5.89 ppm, 4.99 ppm, 2.08 ppm, 1.02 ppm) and *n*-octane (1.3 ppm and 0.92 ppm). iPrOH peaks (3.94 ppm and 1.17 ppm) are visible as well.

tin-oxo cages are not volatile, they do not give rise to any signal in this spectrum. Signals of 1-butene are present, with an extra triplet at 1.02 ppm (–CH_3) which was previously invisible as a result of overlap with tin-oxo cage signals. The signals at 1.3 and 0.9 ppm are also present, showing a much clearer fine structure. This fine structure matches poorly with *n*-butane,[136] but very well with *n*-octane (see Fig. 3.17). The NMR spectrum of *n*-octane is complex as a result of magnetically inequivalent hydrogen atoms. This is seen in both the experimental spectrum and the literature spectrum.[137] No signals for *n*-butane are found; these would show up as two shoulders slightly downfield of the strongest *n*-octane signal.[136] Its presence cannot be completely excluded; if a small amount were present, its NMR signal could be obscured by the *n*-octane peak.

Other photoproduct signals, such as the triplets at 4.49 (1,1-dimethoxybutane) and 3.55 ppm (1-butanol) (see Fig. 3.14), are not visible in the distilled sample. These products could be formed by a reaction with dissolved O_2 (see Fig. 3.2), which was thoroughly removed before DUV exposure in the case of the distilled sample.

To ensure that the formed photoproducts were a result of DUV photoreactions, two blank experiments were performed. First, pure MeOH-d_4 was distilled in the vacuum setup, after which the NMR spectrum was recorded. The only signals that were recorded besides CD_3OH (4.9 ppm) and $CHCD_2OD$ (3.3 ppm) were acetone at 2.2 ppm (which was used for cleaning the setup before the experiments) and a signal at 4.6 ppm. This signal corresponds to an unknown contamination, but certainly not a photoproduct.

Secondly, a non-exposed solution of TinOH in MeOH-d_4 was distilled as well. The only difference with the first blank is the presence of iPrOH, which is also volatile.

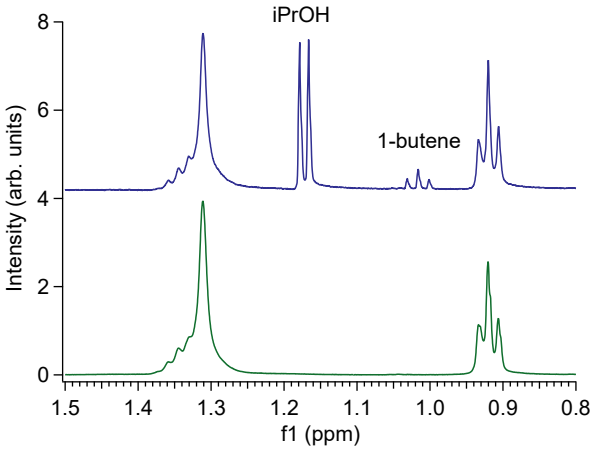

Figure 3.17: 500 MHz ^{1}H NMR spectra, bottom (green): *n*-octane in MeOH-d_4, and TinOH in MeOH-d_4, DUV-exposed for 45 min. and distilled, top (blue). A vertical offset was used on the *y*-axis.

NMR spectra of both blank samples are shown in the ESI (Fig. 9.10).

It should be noted that the NMR analysis of the distilled sample is not very quantitative because no internal standard was added and the amount of distilled iPrOH is unknown. However, with some certainty it can be assumed that more *n*-octane than 1-butene is formed, and that *n*-butane is present only in small quantities if at all.

2D TOCSY NMR

2D TOCSY is a useful method to assign photoproduct signals. The 2D TOCSY spectra after 2.5 h of DUV exposure, zoomed-in on the *n*Bu region and downfield, are shown in Fig. 3.18 and Fig. 3.19 respectively. In the ESI, the couplings are tabulated (Tab. 9.3). Overall, the signals are less well resolved compared to the unexposed sample in Figure 3.7, mainly as a result of broadening of all the *n*Bu peaks. It is notable that all the *n*Bu signals have shifted slightly downfield, with the $Sn_{5/6}$-$\mathbf{CH_2}$-CH_2-CH_2-CH_3 experiencing the largest shift (0.11 ppm for Sn_6 and 0.15 ppm for Sn_5). The shifting of Sn_5-$\mathbf{CH_2}$-CH_2-CH_2-CH_3 resolves this signal from $Sn_{5/6}$-CH_2-CH_2-$\mathbf{CH_2}$-CH_3, which makes it possible to observe that this methylene group appears as a triplet.

The most pronounced new signals after DUV exposure in the downfield region are those of *n*-octane (1.3 and 0.9 ppm) and the two triplets at 4.48 ppm and 3.55 ppm (1,1-dimethoxybutane and 1-butanol). The signals at 1.3 and 0.9 ppm couple with each other, which is consistent with the *n*-octane assignment. Both the 4.48 and 3.55 ppm signals couple with signals overlapping with the Sn_5-CH_2-CH_2-$\mathbf{CH_2}$-CH_3, Sn_6-CH_2-CH_2-$\mathbf{CH_2}$-CH_3 and Sn_6-CH_2-CH_2-CH_2-$\mathbf{CH_3}$ peak.

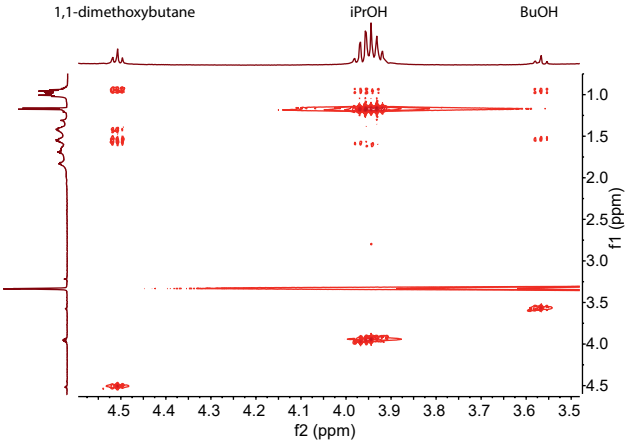

Figure 3.18: Partial 2D TOCSY spectrum of TinOH in MeOH-d_4 after 2.5 h of DUV exposure, zoomed-in downfield.

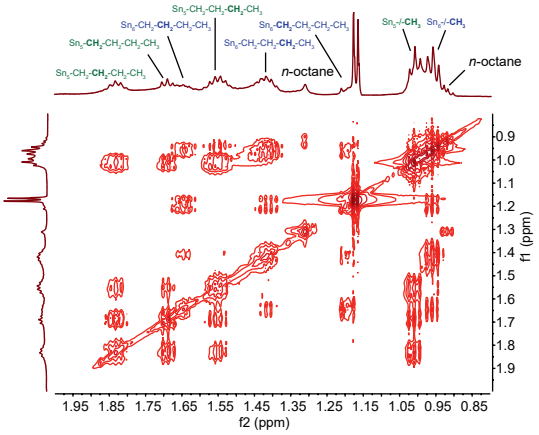

Figure 3.19: Partial 2D TOCSY spectrum of TinOH in MeOH-d_4 after 2.5 h of DUV exposure, zoomed-in on the nBu region. Assignments for the nBu protons are shown as well.

1D selective TOCSY NMR

Recording selective TOCSY spectra is a valuable method to assign signals that are overlapping. For example, except for the 3.55 ppm signal, BuOH proton signals overlap with TinOH nBu signals. Using selective TOCSY and obtaining all couplings to 3.55 ppm, signals at 0.94 ppm (t), 1.38 ppm (sextet), 1.51 ppm (m) and 1.63 ppm are observed. Aside from the signal at 1.63 ppm, this spectrum perfectly matches

a spectrum from BuOH in MeOH-d_4, as shown in Fig. 3.20. The couplings of the amplified signals in the selective TOCSY spectrum match the couplings of BuOH as well. The small peak at 1.63 ppm is probably due to other proton signals that are excited by the 3.55 ppm pulse (see ESI, Fig. 9.11).

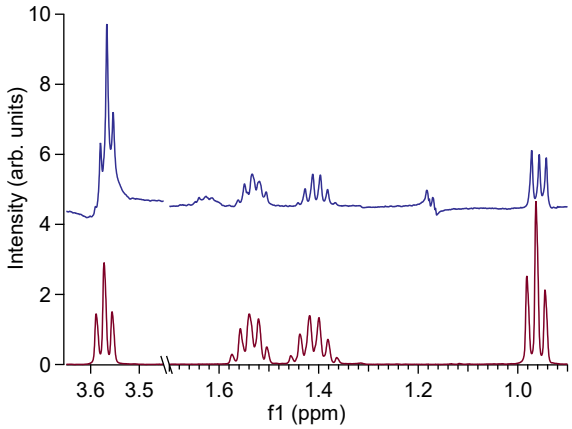

Figure 3.20: Red: BuOH in MeOH-d_4. Blue: Selective TOCSY spectrum of TinOH in MeOH-d_4 after 3.5 h DUV exposure, pulsed at 3.55 ppm. A vertical offset was used on the y-axis.

Signals corresponding to 1,1-dimethoxybutane (acetal of butyraldehyde) also show significant overlap with tin-oxo cage nBu signals, except for the 4.52 ppm signal. The selective TOCSY spectrum that is obtained when pulsed at 4.52 ppm shows similar peaks to the TOCSY spectrum in Fig. 3.20: 0.93 ppm (t), 1.40 ppm (sextet), 1.48–1.58 (overlapping multiplets), as shown in Fig. 3.21. Dissolving butyraldehyde and TinOH in MeOH-d_4 provided a good match with the 1D TOCSY spectrum of 4.52 ppm (see Fig. 3.21). Butyraldehyde reacts with MeOH-d_4 to form the acetal 1,1-dimethoxybutane, as is apparent from the disappearance of the signal at 9.7 ppm (aldehyde proton). This reaction is apparently catalyzed by TinOH, since the aldehyde signal is still present in the red spectrum (butyraldehyde in MeOH-d_4 without TinOH).

A selective TOCSY spectrum was obtained by pulsing at 1.29 ppm (n-octane) as well. The singlet at 1.29 ppm shows a coupling with a triplet at 0.90 ppm (Fig. 3.22), which is consistent with the n-octane assignment. This coupling was also observed in the 2D TOCSY spectrum (see Section 3.3.4).

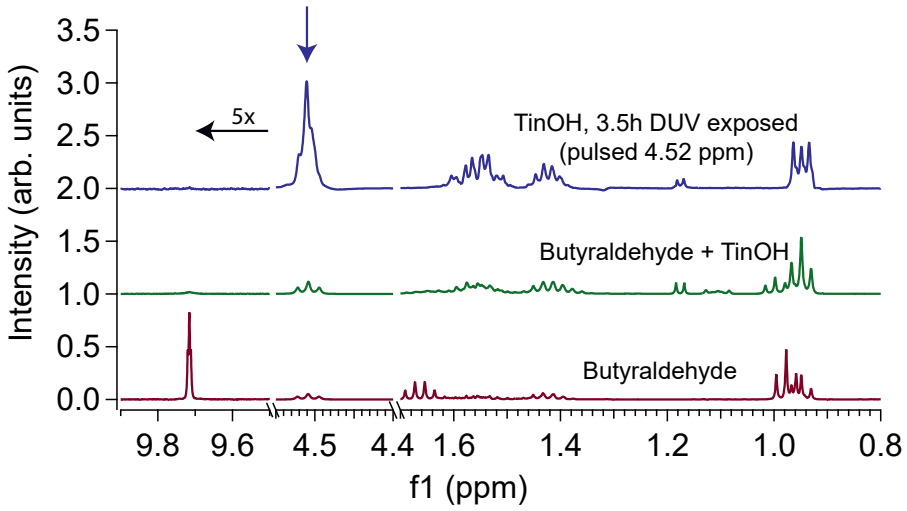

Figure 3.21: Acetal formation in MeOH-d_4, catalyzed by TinOH. Red: NMR spectrum of butyraldehyde in MeOH-d_4. Green: butyraldehyde and TinOH in MeOH-d_4. Blue: selective TOCSY spectrum of TinOH in MeOH-d_4 after 3.5 h DUV exposure, pulsed at 4.52 ppm. A vertical offset was used on the y-axis.

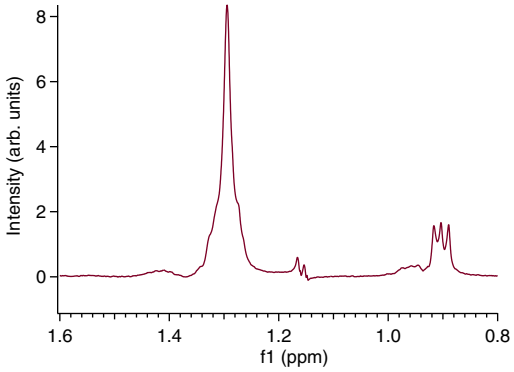

Figure 3.22: Selective TOCSY spectrum of TinOH in MeOH-d_4 after 2.5 h DUV exposure, pulsed at 1.29 ppm.

DOSY NMR

The DOSY spectrum of exposed and unexposed TinOH in MeOH-d_4 is shown in Fig. 3.23. The diffusion coefficient D (f1 axis) of a certain signal is related to its size; smaller molecules diffuse faster. This is described by the Stokes-Einstein equation (Eq. 3.7):

$$R_{\mathrm{H}} = \frac{k_{\mathrm{B}}T}{6\pi\eta D} \tag{3.7}$$

In Eq. 3.7, R_{H} is the hydrodynamic radius (in m), k_{B} is the Boltzmann constant (1.38×10^{-23} m^2 kg s^2 K^{-1}), T is the temperature (in K), η is the viscosity of the solvent (in kg m^{-1} s^{-1}) [MeOH: 5.45×10^{-4}][138] and D is the diffusion coefficient (in m^2 s^{-1}). The hydrodynamic radius is related to the type of solvent and the dynamics of motion and can be viewed as the radius of a hypothetical hard sphere that diffuses with the same speed as the particle under examination.[139] For spheroidal molecules much larger than solvent molecules, R_{H} is considered a good measure for the actual molecular radius.[89]

The value of R_{H} for the tin-oxo cage can be calculated using the diffusion coefficient of the signals corresponding to nBu in the tin-oxo cage material in the DOSY. The four peaks with the lowest log(D) value, at ppm values of 1.83, 1.66, 1.55 and 1.01, were assumed to be the most representative for the diffusion constant. This is because any small impurity in the sample that overlaps in signal with nBu will likely be smaller than the tin-oxo cage. This would shift log(D) to higher values. Additionally, these four signals appear at an almost identical log(D) value. This could mean that these are "clean" signals, without any impurity present that induces signals at the same ppm values. The hydrodynamic radius of the tin-oxo cage, calculated from the average log(D) value of the 4 peaks, is calculated to be 0.78 nm using Eq. 3.7, which is identical to the value reported by Van Lokeren and coworkers.[89]

The 2D DOSY spectrum of TinOH in MeOH-d_4 after 2.5 h DUV exposure (green) is superimposed with the unexposed sample (blue) in Fig. 3.23. The solvent peaks (3.31 ppm and 4.85 ppm) appear at large log(D) values. The peaks in the nBu region are more spread out over multiple log(D) values and appear on average at larger log(D) values in the exposed sample. Since DOSY provides the average diffusion coefficient for one chemical shift and some resonances of small photoproducts overlap with Sn-nBu protons, small photoproducts could significantly shift the measured log(D) to higher values. Although in such cases the intensity vs. gradient strength data can be fitted to a multi-exponential (instead of mono-exponential) decay, obtaining multiple D values, this was not feasible as a result of the limited number of available data points.

The overall shift to higher log(D) values can also be attributed to modifications on the tin-oxo cage itself. For example, a tin-oxo cage in which the nBu chains have been substituted with either –OH or –H would be smaller, giving rise to higher log(D).

The photoproduct signals A (acetal), B (BuOH), C (unknown), D (1-butene) and E (octane/butane) all appear at larger log(D), and therefore smaller R_{H}, than the nBu signals. The R_{H} values for the photoproducts may not be accurate, because the

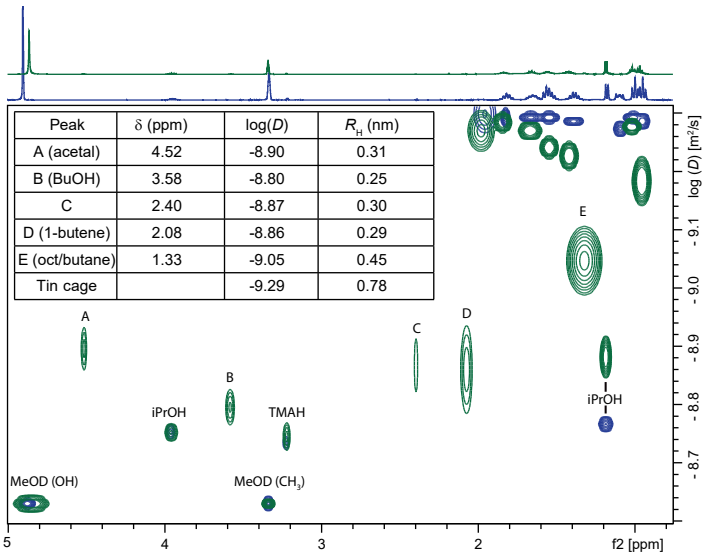

Figure 3.23: 2D DOSY spectra of TinOH in MeOH-d_4. Blue: unexposed. Green: 2.5 h DUV exposed. Product peaks are indicated with capital letters. Inset table shows calculation of the hydrodynamic radius for the product peaks and tin-oxo cage peaks. 1,1-dimethoxybutane is denoted as 'acetal'.

conditions under which the Stokes-Equation applies (spherical molecule of much larger size than the solvent molecules) do not hold. Still, the small size of these molecules is unequivocal. The signals A, B, C, D and E clearly correspond to small photoproducts rather than functional groups that are attached to the tin-oxo cage (for instance a Sn-O-CH_2-CH_2-CH_2-CH_3 group).

Quantitative NMR

In the previous sections, we have assigned signals in the ^{1}H NMR spectrum to photoproducts. Formation of these photoproducts was not yet quantified, however. ^{1}H NMR spectroscopy inherently contains a method for quantification, because peak areas can be a reliable measure for the relative amount of a chemical species. Because the starting amount of tin-oxo cage (in g or in mol) is known, this can be converted to an amount of converted material or to amounts of formed photoproducts.

The quantitative measurements were performed in a quartz NMR tube instead of a quartz cuvette. This has the advantage that sample transfer (from cuvette to NMR tube) need not take place, limiting oxidation and evaporation effects.

^{1}H NMR spectra at different exposure times are shown in Fig. 3.24. The signals in the *n*Bu region are less broadened compared to the ^{1}H NMR spectra at different exposure times when irradiated in a quartz cuvette (Fig. 3.14). Furthermore, photo-

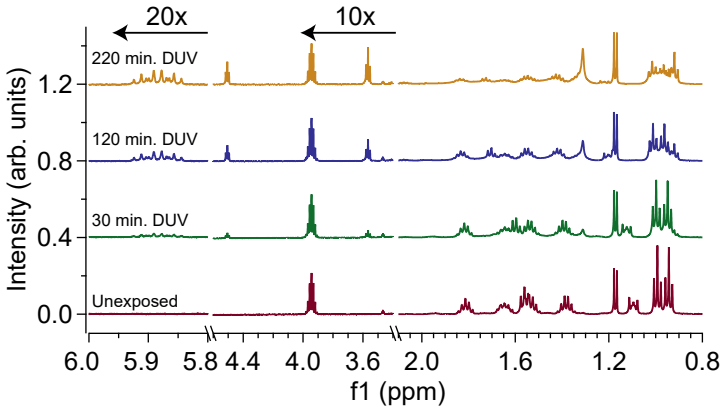

Figure 3.24: Zoomed-in ^{1}H NMR spectra (500 MHz) of TinOH in MeOH-d_4 after multiple DUV exposure times, performed in a quartz NMR tube. From bottom to top: 0 h (red), 30 min. (green), 120 min. (blue) and 220 min. (purple) DUV exposure. A vertical offset was used on the y-axis. The spectra were normalized to the iPrOH C–H peak at 3.95 ppm.

product peaks (especially 1-butene) are sharper.

For a quantitative analysis, we first need to consider solubility of the photoproducts. Material that is above the solubility threshold will not appear in the NMR spectra; especially gases can easily escape. Although butane and 1-butene are both gases at standard temperature and pressure, their solubility in methanol is considerable: both around 4 mol%.[140,141] In the ESI (Section 9.3.2), it is shown that this is more than sufficient for dissolution of all formed butane or 1-butene.

iPrOH was used as internal standard for this measurement. iPrOH is present in TinOH powder because it is part of its crystal structure.[107] The septet at 3.95 ppm (C–H) is well isolated from photoproduct and Sn-nBu signals. By comparing the intensity of other peaks to this iPrOH peak, the amount of generated products (in mol) and the loss of Sn-nBu can be calculated. This is shown in the ESI (Section 9.3.2).

A clear difference with the quartz cuvette measurement is that the signals for n-octane at 1.3 ppm and 0.9 ppm are much more prominent for the quartz NMR tube measurement (compare e.g. Fig. 3.24 with Fig. 3.14). This can be explained by the smaller involvement of oxygen in the reaction; the NMR tube remained closed at all times whereas the cuvette was opened several times to take aliquots. If oxygen is present in lower concentrations, butyl radicals are more likely to react with other butyl groups attached to the tin-oxo cage (see Fig. 3.3).

Product peaks increase upon exposure while peaks corresponding to Sn–nBu decrease. This can be quantified by peak integrals. For most product peaks this is straightforward, but for n-octane the signal overlaps with Sn_6-CH_2-CH_2-$\mathbf{CH_2}$-CH_3 (see Fig. 3.25). Additional issues are a non-constant baseline and a downfield shift

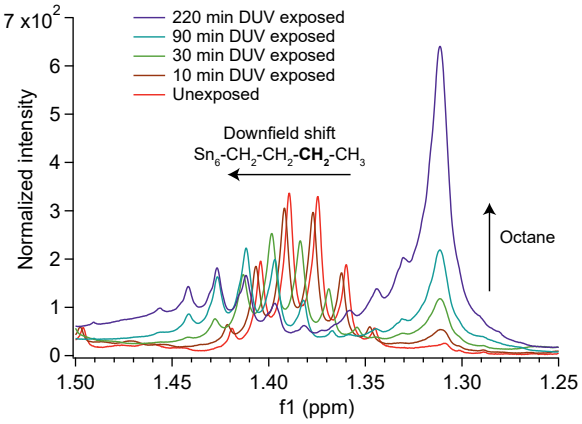

Figure 3.25: Evolution of octane and decrease and downfield shift of the 1.38 ppm signal (Sn_6-CH_2-CH_2-$\mathbf{CH_2}$-CH_3) upon DUV exposure. All spectra were normalized to the iPrOH C–H peak at 3.95 ppm.

of (especially) the Sn_6-*n*Bu signals. This complicates quantification of *n*-octane formation and loss of Sn_6-*n*Bu. An approximation for these effects was made as follows. First, the baseline was corrected by correcting for the slope between approximately 1.48 ppm (downfield from both signals) and 1.26 ppm (upfield from both signals). *n*-octane formation was quantified by calculating the integral between 1.32 and 1.28 ppm (no overlap). This was multiplied by the ratio between the complete peak area (1.375–1.26 ppm) and the area between 1.32 and 1.28 ppm. This ratio was calculated using the 220 min. exposed spectrum, which has negligible overlap between the Sn_6-*n*Bu and *n*-octane signals. A baseline (complete peak area 1.32–1.28 ppm at $t = 0$, resulting from small impurities in the MeOH-d_4) was subtracted from the resulting area values.

For the Sn_6-CH_2-CH_2-$\mathbf{CH_2}$-CH_3 signal, the integral was taken between the middle of the signal (as determined by the minimum of the sextet structure) and 0.04 ppm downfield from it (end of sextet structure). This downfield half of the peak has no significant overlap with the *n*-octane signal. The full peak integral was calculated by multiplying with 2. This integral was used to track loss of Sn_6-*n*Bu.

For the other peaks, calculation of peak integrals was more straightforward. All other photoproducts give rise to at least one peak that does not significantly overlap with the Sn-*n*Bu signals: 1-butene at 5.9 ppm, 1,1-dimethoxybutane at 4.5 ppm, BuOH at 3.55 ppm, and butyraldehyde at 2.4 ppm. The amount of Sn_5-*n*Bu was determined using the peak at 1.82 ppm (Sn_5-CH_2-$\mathbf{CH_2}$-CH_2-CH_3). Although this peak also undergoes downshift, and a correction for the baseline was necessary, this peak does not significantly overlap with any known photoproducts.

In Fig. 3.26, the amount of formed products is plotted vs. exposure time. It can be seen that photoproduct formation scales approximately linearly with exposure time; there is no evidence that formation of any product occurs via a secondary mechanism

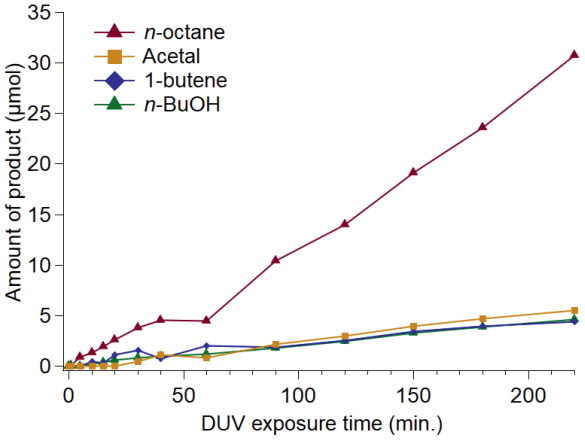

Figure 3.26: Amount of product arising from the DUV photochemistry of TinOH (8.5 µmol in 0.6 mL MeOH-d_4), as a function of exposure time.

Table 3.2: Yield of the five most important photoproducts (in µmol), starting from an 8.2 µM solution of TinOH. Rate of formation is shown (as calculated by linear fit), as well as selectivity (assuming no other product formation). 1,1-dimethoxybutane is denoted as 'acetal'.

	1-butanol	Acetal	1-butene	Butyraldehyde	*n*-octane
10 min.	0.22	0	0.43	0	2.76
30 min.	0.86	0.43	1.58	0	7.61
90 min.	1.79	2.15	1.86	0.14	21.1
220 min.	4.66	5.59	4.44	0.57	62.2
Rate (nmol/min.)	21.0	26.7	20.1	2.62	133
Selectivity	10.3%	13.1%	9.9%	1.3%	65.4%

(i.e. a photoproduct is converted by DUV into a secondary product). Fluctuations can be attributed to either statistical errors (signal to noise ratio of the NMR spectrum) or systematic errors such as insufficient homogeneity of the measured solution. Clearly, the main formed product is *n*-octane; the other products are formed in much lower quantities (see Table 3.2).

The quantitative analysis can also be used for measuring conversion of Sn_5-*n*Bu and Sn_6-*n*Bu. Some complications arise, however. The area of the Sn_5-CH_2-$\mathbf{CH_2}$-CH_2-CH_3 peak (1.81 ppm) is not equal to that of Sn_6-CH_2-CH_2-$\mathbf{CH_2}$-CH_3 (1.41 ppm), even without photo-exposure. This is possibly due to differences in the relaxation time T_1.[142] As a result, it was difficult to accurately quantify loss of Sn-*n*Bu. Therefore, a "relative loss" of Sn_5-*n*Bu and Sn_6-*n*Bu was calculated by dividing areas of 1.81 ppm and 1.41 ppm peaks with their values at $t = 0$. This is shown in Fig. 3.27a. In

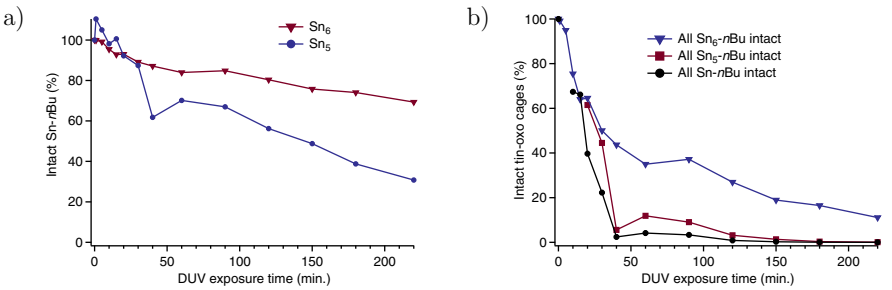

Figure 3.27: (a) Relative loss of Sn_5-*n*Bu (blue) and Sn_6-*n*Bu (red), as calculated from 1.81 ppm and 1.41 ppm peak areas. (b) Amount of intact tin-oxo cages: tin-oxo cages with all Sn_6-*n*Bu intact (blue), tin-oxo cages with all Sn_5-*n*Bu intact (red), and tin-oxo cages with all Sn-*n*Bu intact (black).

contrast with predictions,[103] the Sn–C cleavage appears to take place predominantly at the 5-coordinated site.

To calculate the chance P that a TinOH molecule has lost *at least one* 5-*n*Bu chain, we need to consider that this chance is equal to one minus the chance that it has lost *no* 5-*n*Bu chains ($P_{\text{no 5-butyl loss}}$). If we assume that all cleavage events are independent, $P_{\text{no 5-butyl loss}}$ is equal to the chance that one particular 5-*n*Bu chain is cleaved off to the power of six (because there are six butyl groups bound to 5-coordinated tin). This is described in Eq. 3.8. This equation is valid under the assumption that each Sn–C cleavage is random (i.e. does not depend on whether a previous Sn–C cleavage has taken place on the same tin-oxo cage). The chance that one particular butyl group is cleaved is then equal to the total fraction of cleaved butyl groups in the entire population of tin-oxo cages.

$$P_{\text{at least one 5-butyl loss}} = 1 - P_{\text{no 5-butyl loss}} = 1 - \left(\frac{N_{\text{5-butyl non-cl.}}}{N_{\text{5-butyl initial}}}\right)^6 \tag{3.8}$$

In Eq. 3.8, $N_{\text{5-butyl initial}}$ is the total initial number of 5-butyl chains in the entire population of tin-oxo cages. $N_{\text{5-butyl non-cl.}}$ is the total number of 5-butyl chains (in the entire population) that have not been cleaved off. Obviously, the same equation applies to the loss of 6-butyl chains. The results are shown in Fig. 3.27b, which shows the relative amount of intact tin-oxo cages. It can be seen that after 50 minutes of DUV exposure, almost no intact tin-oxo cages remain, even though the majority of *n*Bu groups have not yet been cleaved off (see Fig. 3.27a).

The quantum yield (Φ) of Sn–C cleavage can be measured as well. Φ was defined by the number of cleaved Sn–C bonds (calculated from photoproduct signals) divided by the number of absorbed photons. The number of absorbed photons was calculated by dividing the total amount of energy for a certain exposure time by the energy of a DUV photon (8.8×10^{-19} J). It was assumed that all light from the laser pulses was absorbed.

The amount of converted Sn_5-*n*Bu and Sn_6-*n*Bu as calculated by the 1.41 and

1.81 integrals (see Fig. 3.27a) may not be completely accurate. As discussed before, their initial values are already different. Therefore, it may be better to calculate the quantum yield by using the photoproduct signals. As a measure for the quantum yield, it is most accurate to use the reaction rate (in mol/min.), which was obtained by fitting the lines in Fig. 3.26 to linear functions. It was found that approximately 0.23 µmol of photoproduct was formed per minute of DUV exposure. If we convert this to the number of Sn–C cleavage events per number of photons, and assume that *n*-octane is formed by only one cleaved butyl, we obtain a quantum yield of around 20% for Sn–C cleavage. This is significantly lower than the quantum yield found by the UV-Vis spectroscopy experiments in methanol (60–70%, see Section 3.3.1). This is probably due to reflection losses, which lead to an overestimation of the number of absorbed photons. The used NMR tube (5 mm) was slightly smaller than the laser spot, and reflection losses occur on the cylindrical NMR tube.

Formation of *n*-octane can occur either through simple combination of two butyl radicals, or by butyl abstraction from another Sn–Bu (see Scheme 3.3). Given the high quantum yield, the latter appears to be more probable. In this scenario, only one photo-induced Sn–Bu cleavage would be required to yield one *n*-octane molecule.

3.4 Conclusion

In this chapter, the DUV photochemistry of TinOH and TinA was studied in solution. Clearly, Sn–C cleavage is the dominant photoreaction upon DUV photon absorption on tin-oxo cages. In UV/Vis experiments, the initial quantum yield of this cleavage was estimated to be 60–80%.

The nature of the Sn–C cleavage was studied using a spin trapping experiment. The molecule TEMPO (containing an unpaired electron) induces a paramagnetic shift on the chemical shift of a reference compound. This paramagnetic shift decreased upon DUV exposure of a TEMPO+TinOH solution, indicating a decrease in the concentration of TEMPO. This decrease was induced by a chemical reaction between TEMPO and butyl radicals. This proves that the Sn–C cleavage is homolytic, producing a butyl radical and a tin-centered radical. Formation of a TEMPO-butyl adduct, visible in the NMR spectrum, formed additional proof of this photoreaction. Photoproducts were further studied using NMR spectroscopy. In the 1D ^{1}H NMR spectrum of DUV exposed TinOH in MeOH-d_4, several new signals appeared, corresponding to photoproducts. Diffusion-ordered (DOSY) NMR showed that these signals corresponded to small molecules, rather than functional groups attached to the tin-oxo cage. Using total correlation NMR spectroscopy (TOCSY), the signals were assigned to *n*-octane, 1-butene, 1-butanol and 1,1-dimethoxybutane. Formation mechanisms for these products are proposed (see Scheme 3.4).

When the solution of TinOH was degassed before DUV exposure and the solution was distilled, only *n*-octane and 1-butene were found in the NMR spectrum. This indicates that the other products (1-butanol and 1,1-dimethoxybutane) are formed by reaction with dissolved oxygen. No signals for *n*-butane could be seen, which means that it is probably formed only in low quantities. This is quite different from EUV photochemistry in thin tin-oxo cage films, where *n*-butane and 1-butene are major products, and *n*-octane is minor.[111]

The formation of products was quantified using the NMR peak areas. Production of *n*-octane was found to be by far the most prominent photoreaction (65% selectivity). *n*-Octane can be formed by recombination of two *n*-butyl radicals or by abstraction of a butyl group from the cage by a butyl radical. The generation rate of *n*-octane was found to be much higher for a sample that was irradiated in a quartz NMR tube instead of a cuvette. Less involvement of oxygen is a possible reason for this. The quantum yield was found to be around 20%, which is however a lower bound because reflection losses are not taken into account.

This chapter shows that radical chemistry plays a major role in the initial photoreaction. Initially formed radicals can either recombine or react further. Possible intermediates are tin (II) and Sn–H. In the solid state, the quantum yield was generally found to be lower than the results shown in this chapter.[111] This can be attributed to the formation of a "radical cage pair", which is much more stable in a solid film than in solution. Inhibiting recombination of the Sn·/C· caged pair could drastically increase the sensitivity of organometallic photoresist materials in thin films.

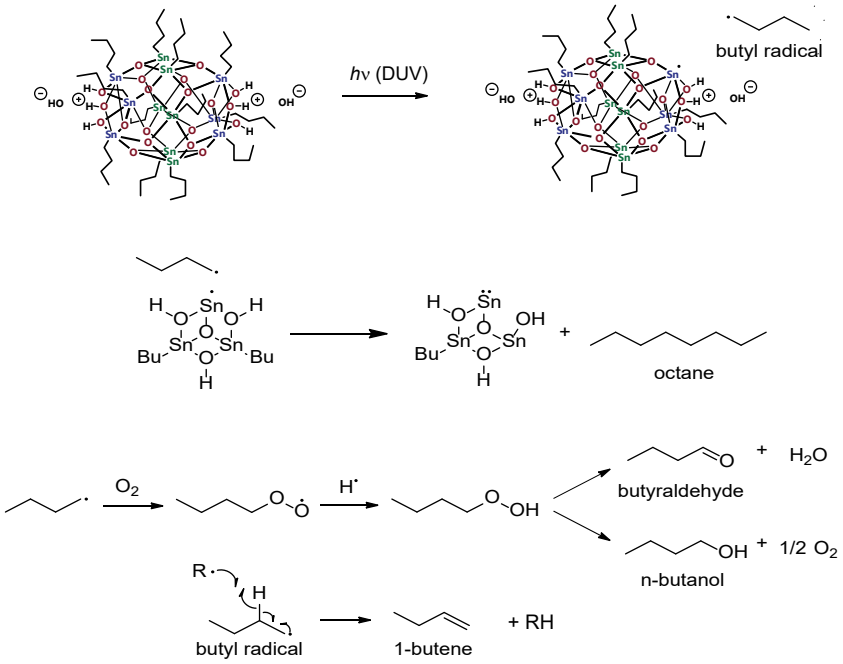

Scheme 3.4: Photoreaction scheme describing formation of photoproducts upon DUV exposure of a TinOH solution in MeOH-d_4.

3.5 Acknowledgments

The author acknowledges Jan Meine Ernsting, Eline van den Heuvel, Michiel Hilbers, Xander Schaapkens, Daniel Smith and Janita Vermeulen for their contribution to this work.